Metal Artifact Reduction With MAVRIC SL at 3-T MRI in Patients With Hip Arthroplasty

Soo-Jung Choi[1], **Kevin M. Koch**[2], **Brian A. Hargreaves**[3,4], **Kathryn J. Stevens**[3,4], and **Garry E. Gold**[3,4]

[1]Department of Radiology, Asan Foundation, Gangneung Asan Hospital, University of Ulsan, College of Medicine, Gangneung-si, Gangwon-do, Korea

[2]Applied Science Laboratory, GE Healthcare, Waukesha, WI

[3]Department of Radiology, Richard M. Lucas Center for Imaging, Stanford University School of Medicine, 300 Pasteur Dr, Grant Bldg S0-68B, Stanford, CA 94305-5105

[4]Department of Radiology, Stanford Hospital and Clinics, Redwood City, CA

Abstract

OBJECTIVE—The objective of our study was to compare the multiacquisition variable-resonance image combination selective (MAVRIC SL) sequence with the 2D fast spin-echo (FSE) sequence for metal artifact reduction on 3-T MRI in patients with hip arthroplasty (HA).

MATERIALS AND METHODS—Matched 2D FSE and MAVRIC SL images of 21 hips (19 patients with HA) were included in the study group. Paired image sets, composed of 13 coronal and 12 axial slices (total, 25 image sets), of the 21 hips were evaluated. For quantitative analysis, the artifact area was measured at the level of the hip and femur. For qualitative analysis, two musculoskeletal radiologists independently compared paired 2D FSE and MAVRIC SL sets in terms of artifacts, depiction of anatomic detail, level of diagnostic confidence, and detection of abnormal findings.

RESULTS—The measured artifact area was significantly smaller ($p < 0.05$) on MAVRIC SL than 2D FSE at both the level of hip (59.9% reduction with MAVRIC SL) and femur (31.3% reduction with MAVRIC SL). The artifact score was also significantly decreased ($p < 0.0001$) with MAVRIC SL compared with 2D FSE for both reviewers. The hip joint capsule and the tendon attachment sites of the obturator externus and iliopsoas muscles were better depicted with MAVRIC SL than 2D FSE ($p < 0.0125$). Abnormal findings were significantly better shown on MAVRIC SL imaging compared with 2D FSE imaging ($p < 0.0001$).

CONCLUSION—The MAVRIC SL sequence can significantly reduce metal artifact on 3-T MRI compared with the 2D FSE sequence and can increase diagnostic confidence of 3-T MRI in patients with total HA.

Address correspondence to G. E. Gold (gold@stanford.edu)..

Keywords

arthroplasty; hip; MR artifact; MRI

Hip arthroplasty (HA) is one of the most commonly performed procedures in the aging population. Approximately 1–3% of the older adult population (65 years) in the United States will undergo total HA at some point [1]. In recent years there have been marked improvements in component design and the surgical technique of HA, but patients continue to have postoperative complications after hip replacement, which can require revision or implant removal. Over time, HAs can be affected by periprosthetic osteolysis and loosening as a result of wear-induced synovitis [2]. Therefore, there has been a demand for imaging modalities that can provide an accurate postoperative assessment after HA. Thanks to its superior soft-tissue contrast and metal artifact reduction, MRI has been found to be the most accurate imaging tool in the assessment of periprosthetic osteolysis, wear-induced synovitis, and periarticular neurovascular abnormalities in patients with symptomatic HA [3-9]. MRI has also been recognized as an appropriate assessment tool for patients with adverse local tissue reaction, otherwise known as aseptic lymphocytic vasculitis–associated lesions (ALVAL) or adverse reactions to metal debris in the setting of metal-on-metal (MOM) total hip arthroplasty (THA) [10-16]; however, these studies were conducted with only 1.5-T MR systems because the degree of susceptibility artifact increases at higher magnetic field strengths. Many imaging centers have only 3-T MR systems, creating increased demand for new metal artifact reduction techniques for 3-T MR scanners.

Multiacquisition with variable resonance image combination (MAVRIC) and slice-encoding metal artifact correction (SEMAC) are two recently developed metal artifact reduction techniques that significantly reduce susceptibility artifacts near metallic hardware [8, 17-19]. MAVRIC selective (MAVRIC SL) uses frequency-selective excitation with multiple ranges of different frequency bands. It minimizes image distortion and provides a high signal-to-noise ratio (SNR) by combining multiple individual spectral bin images acquired from different frequency bands. However, through-plane aliasing artifact can occur due to lack of Z-selectivity [8, 17, 20]. On the other hand, SEMAC uses multislice excitation through the use of a slice selection gradient, and view angle tilting is applied to avoid in-plane artifacts [9, 17, 20, 21]. Consequently, SEMAC retains slab selectivity along the *z*-axis, unlike MAVRIC, but requires longer scanning times to preserve high SNR [17, 20, 21]. MAVRIC SL possesses advantageous elements of both techniques by retaining the slab selectivity (Z-selectivity) of SEMAC by way of a Z gradient and by retaining the higher SNR of MAVRIC by way of an overlapped spectral strategy with multiple frequency-selective excitation [17]. MAVRIC SL has been shown to improve visualization of the ankle in a patient with orthopedic hardware in place [17]. However, no studies investigating metal artifact reduction with 3-T MRI in HA patients have been described in the published literature to our knowledge.

The purpose of this study was to compare the MAVRIC SL technique with the conventional 2D fast spin-echo (FSE) technique for the reduction of metal artifacts on 3-T MRI of patients with HA.

Materials and Methods

Patients

Institutional review board approval was obtained for this HIPAA-compliant study, and informed consent was waived. From January 2010 to February 2013, 3-T MRI of the hip including MAVRIC SL was performed of 48 consecutive patients (male-to-female ratio = 17:31; mean age, 60.9 years; age range, 42–84 years) with HA. Nineteen of the 48 patients who underwent 2D FSE and MAVRIC SL imaging in the same imaging planes and sequences were included in this study. Two of them underwent bilateral hip MR examinations. Therefore, a total 21 hips in 19 patients with matching 2D FSE and MAVRIC SL sequences in the same imaging planes were included in the study (male-to-female ratio = 7:12; mean age, 60.8 years; age range, 45–84 years). Of the 21 hips, 14 had MOM THA, four had metal-on-polyethylene THA, one had resurfacing arthroplasty, and two had hemiarthroplasties.

MR Acquisition

All MR examinations were performed on a 3-T MR system (GE Healthcare, Waukesha, WI, USA) with an eight-channel cardiac coil. Imaging was performed with a combination of 2D FSE and MAVRIC SL sequences using similar slice thicknesses and spacing. The MR examinations were performed with different FOVs and contrast settings depending on the specific clinical questions asked.

Two-dimensional FSE images were obtained in at least two orthogonal planes mixed with the following sequences: T1-weighted, T2-weighted or T2-weighted IDEAL (iterative decomposition of water and fat with echo asymmetry and least-squares estimation), proton density–weighted, and STIR images. The 2D FSE sequence was optimized for imaging near metal using a ± 27.7 kHz bandwidth to reduce susceptibility artifacts. The 2D FSE proton density–weighted imaging sequence was performed with the following parameters: TR/TE range, 3000/29–32; bandwidth, ± 127.7 kHz; FOV, various; number of acquisitions, 1; acquisition matrix, 384 × 224; echo-train length (ETL), 8; slice thickness, 4–5 mm; spacing, 4–6 mm; and acquisition time, 3–5 minutes. The 2D FSE STIR sequence was performed with following parameters: TR range/TE range, 4100–5750/34–52; bandwidth, ± 127.7 kHz; FOV, various; number of acquisitions, 1–2; inversion time, 170 seconds; acquisition matrix, 256–320 (frequency) × 192 (phase); ETL, 6–12; slice thickness, 3–5 mm; spacing, 3–5 mm; and acquisition time, 6–7 minutes.

MAVRIC SL proton density–weighted images were acquired in either the coronal or axial plane using the following parameters: TR range/TE range, 3000–4300/35–37; bandwidth, ± 127.7 kHz; ETL, 20; FOV, various; number of acquisitions, 0.5; acquisition matrix, 288 (frequency) × 192 (phase); slice thickness, 4 mm; and spacing, 3–5 mm. The imaging parameters for the MAVRIC SL inversion recovery (IR) sequence were as follows: TR range/TE range, 4000–8700/35–36; bandwidth, ± 127.7 kHz; ETL, 20; inversion time, 150–170 seconds; acquisition matrix, 288 (frequency) × 192 (phase); slice thickness, 4–5 mm; and spacing, 4–5 mm. The MAVRIC SL images were acquired using 2.25-kHz spectral bins (number of MAVRIC spectral bins, 24) separated by 1 kHz and were reconstructed using

bin overlap deblurring [17] followed by sum-of-squares combination of the spectral bins (hybrid Z slap, 1.0). The acquisition time for each MAVRIC SL sequence was 6–10 minutes.

The following paired 2D FSE and MAVRIC SL images were used for image analysis: 20 MAVRIC SL IR images were matched with 2D FSE STIR images and five MAVRIC SL proton density–weighted imaging were matched with 2D FSE proton density–weighted imaging in the same imaging plane. These 25 matched 2D FSE and MAVRIC SL imaging sets obtained from a total of 21 hip MRI examinations consisted of 13 coronal and 12 axial slices.

Quantitative Image Analysis

For quantitative image analysis, the area of metal artifact around the implant was measured on the paired coronal and axial 2D FSE and MAVRIC SL images using a slice through the center of the implant. All measurements were performed by one musculoskeletal radiologist using a Centricity PACS (GE Healthcare). An ROI was drawn around the artifact encompassing the signal void (including the implant) and the surrounding image distortion and signal pile-up. The total area of artifact was measured separately on both the acetabular side (acetabulum and hip joint) and the femoral side (femoral stem area). On coronal imaging sets, a perpendicular line was drawn through the basicervical femoral neck at the slice through the center of the implant. The area of artifact on the hip side was defined by drawing an ROI around artifact above that line, so the hip joint and acetabulum were included. The area of artifact on the femoral side was measured by drawing an ROI around artifact distal to the line (Fig. 1). On axial image sets, the artifact area of the hip was measured on a slice level with the top of the femoral head, where the acetabular implant was most visible. Artifact on the femoral side was measured at the level of lesser trochanter. The mean areas of artifact measured around the hip and femur on paired 2D FSE and MAVRIC SL images were compared using a paired Student $t$test. The mean artifact areas around the hip and femur were also compared between the patients with MOM THA and those with metal-on-polyethylene THA using a Mann-Whitney test.

Qualitative Image Analysis

For qualitative image analysis, two fellowship-trained musculoskeletal radiologists (14 and 16 years of experience in musculoskeletal radiology) independently evaluated and compared the paired 2D FSE and MAVRIC SL sequences and imaging sets for artifacts, depiction of anatomic detail, level of diagnostic confidence, and detection of abnormal findings.

For artifact comparison, visualization of the bone-metal interface and the extent of artifact were assessed on all the images in the 2D FSE and MAVRIC SL sets. The artifact was evaluated separately on the acetabular side and the femoral side in the same manner as the aforementioned quantitative analysis method. The degree of artifact was scored using the following 5-point scale: 1, normal or barely visible artifact; 2, visible artifact but a well-visualized bone-metal interface; 3, mild artifact with mildly impaired visualization of the bone-metal interface; 4, moderate artifact with moderately impaired visualization of the bone-metal interface; and 5, severe artifact and nonvisualization of the bone-metal interface.

For the depiction of anatomic detail, the capsule of the hip and the tendon attachment sites were evaluated. Visualization of the medial and lateral joint capsule of the hip was recorded on coronal imaging sets, and visualization of either the anterior or posterior joint capsule was recorded on axial imaging sets. Tendon attachment sites were evaluated on the lateral and inferior aspects of the hip. Visualization of the gluteus medius and minimus tendon insertions into the greater trochanter was evaluated on both the coronal and axial imaging sets. The tendon attachment sites of the obturator externus and iliopsoas muscles were assessed on the coronal and axial images, respectively, for evaluation of image quality over the inferior aspect of the hip. The following 3-point scale was used for the depiction of anatomic structures: 1, tendon insertion or tendon abnormality well depicted with no diagnostic impairment; 2, partially depicted tendon attachment or suspected tendon abnormality with mild to moderate diagnostic impairment; and 3, nonvisualization of tendon attachments.

For evaluation of diagnostic confidence, the level of overall diagnostic confidence was independently scored on 2D FSE and MAVRIC SL imaging sets. The level of diagnostic confidence was scored using the following 5-point scale: 1, diagnostic confidence is higher on 2D FSE than MAVRIC SL; 2, no difference between 2D FSE and MAVRIC SL; 3, diagnosis can be made on 2D FSE but is better seen on MAVRIC SL; 4, diagnosis cannot be made on 2D FSE but can be made on MAVRIC SL with mild to moderate confidence; and 5, diagnosis cannot be made on 2D FSE but can be confidently made on MAVRIC SL.

For evaluation of abnormal findings, two reviewers independently analyzed the matched 2D FSE and MAVRIC SL image sets to see whether the following abnormal findings were present on either sequence: acetabular osteolysis, femoral periprosthetic loosening, joint effusion, extraarticular fluid collection or mass, extraarticular fluid collection with communication with the hip joint, tumorlike lesion, and high-grade muscle or tendon tear. Any additional abnormal findings were also recorded. Osteolysis was denoted as intermediate-to high-signal-intensity replacement of bone marrow adjacent to the acetabulum or proximal femur. Femoral periprosthetic loosening was defined as linear fluid signal intensity in the bone-metal interface surrounding the prosthesis. A muscle or tendon tear was recorded only if there was a high-grade tear. Fatty infiltration or atrophy of the muscle was not included as an abnormal finding.

Statistical Analysis

Differences between measured areas of artifacts (quantitative data) on 2D FSE and MAVRIC SL were assessed using a paired Student t test, with $p < 0.05$ indicating statistical significance. A Mann-Whitney test was used to compare differences of measured artifact areas between patients with metal-on-polyethylene THA and patients with MOM THA. Qualitative data, including scores of artifacts and the depiction of anatomic detail, were analyzed with a Wilcoxon signed rank test. For the scores of artifacts, $p < 0.05$ was considered to indicate statistical significance. For multiple comparisons for the depiction of anatomic detail, $p < 0.0125$ was considered to indicate a statistical significance after Bonferroni correction. Differences in the detection of abnormal findings between 2D FSE and MAVRIC SL were analyzed using a McNemar test, with $p < 0.05$ indicating statistical

significance. Interobserver agreement for the scoring of artifacts, depiction of anatomic detail, level of diagnostic confidence, and detection of abnormal findings was calculated using kappa statistics; a kappa value has a maximum of 1.0 when agreement is perfect, whereas a kappa value of 0 indicates agreement that is no better than chance agreement. The kappa values of this study were interpreted according to the guidelines of Landis and Koch [22]. The strength of agreement quantified by a kappa statistic was graded as follows: < 0, poor; 0.01–0.20, slight; 0.21–0.40, fair; 0.41–0.60, moderate; 0.61–0.80, substantial; and 0.81–0.99, almost perfect. All statistical analyses were performed using statistical software (MedCalc, version 10.4.0.0, MedCalc Software).

Results

Quantitative Analysis

The mean artifact areas of the hip and femur were significantly decreased with MAVRIC SL compared with 2D FSE ($p < 0.05$) (Fig. 2). The overall mean artifact area on the hip side was 8596 ± 4179 mm^2 (SD) on 2D FSE and 3130 ± 1217 mm^2 on MAVRIC SL. The mean artifact reduction using MAVRIC SL was therefore 59.9% ($p < 0.0001$) on the hip side. The mean artifact area on the femoral side was 2722 ± 2227 mm^2 on 2D FSE and 1517 ± 913 mm^2 on MAVRIC SL. The mean artifact reduction using MAVRIC SL was 31.3% ($p = 0.0024$) on the femoral side.

The artifact area of the hip on MAVRIC SL was significantly smaller on both the coronal and axial imaging sets compared with 2D FSE (coronal 2D FSE = 6659 ± 2521 mm^2; coronal MAVRIC SL, 2858 ± 1207 mm^2; axial 2D FSE, $10,693 \pm 4684$ mm^2; axial MAVRIC SL, 3425 ± 1209 mm^2) ($p < 0.0001$). The artifact area of the femur on MAVRIC SL was significantly smaller on coronal imaging sets compared with 2D FSE (coronal 2D FSE, 3375 ± 1217 mm^2; coronal MAVRIC SL, 2114 ± 695 mm^2) ($p = 0.0018$). There was no significant difference in terms of artifact area of the femur on axial imaging sets between 2D FSE and MAVRIC SL (axial 2D FSE, 2013 ± 2856 mm^2; axial MAVRIC SL, 869 ± 643 mm^2) ($p = 0.1168$) (Fig. 2).

The mean artifact area of the hip was significantly larger in patients with MOM THA on both 2D FSE and MAVRIC SL than in patients with metal-on-polyethylene THA (MOM THA group, 9638 ± 3911 mm^2 on 2D FSE and 3451 ± 1144 mm^2 on MAVRIC SL; metal-on-polyethylene THA group, 4299 ± 1532 mm^2 on 2D FSE and 1924 ± 542 mm^2 on MAVRIC SL) ($p < 0.005$). There was no statistically significant difference in the mean artifact areas of the femur on 2D FSE and MAVRIC SL between the two groups (MOM THA group, 2664 ± 2191 mm^2 on 2D FSE and 1472 ± 862 mm^2 on MAVRIC SL; metal-on-polyethylene THA group, 2073 ± 1157 mm^2 on 2D FSE and 1731 ± 1094 mm^2 on MAVRIC SL) ($p > 0.05$).

Qualitative Analysis

The overall mean artifact scores on the hip and the femoral sides were significantly lower with MAVRIC SL compared with 2D FSE for both reviewers ($p < 0.001$) (Fig. 1). Interobserver agreement for scores of artifact was substantial ($\kappa = 0.792$). The mean artifact

score was significantly decreased with MAVRIC SL compared with 2D FSE on both the coronal and axial imaging sets for both reviewers ($p < 0.05$) (Table 1).

For the depiction of anatomic detail, the evaluated anatomic structures near the hip joint were better depicted on MAVRIC SL compared with 2D FSE (Table 2). In particular, the joint capsule of the hip and the tendon attachment sites of the obturator externus on coronal imaging and of the iliopsoas tendon on axial imaging were significantly better seen on MAVRIC SL than on 2D FSE ($p < 0.0125$). There was no significant difference for the depiction of the gluteus medius tendon attachment site on both of coronal and axial imaging sets and for the depiction of the gluteus minimus attachment site on coronal imaging between 2D FSE and MAVRIC SL for one of the two reviewers ($p > 0.125$). Interobserver agreement for the depiction of anatomic detail was substantial ($\kappa = 0.622$).

The mean level of diagnostic confidence was 4.20 ± 0.76 for reviewer 1 and 4.32 ± 0.69 for reviewer 2 (Figs. 3 and 4). Interobserver agreement for the level of diagnostic confidence was substantial ($\kappa = 0.737$).

The number of detected abnormal findings was significantly greater on MAVRIC SL than on 2D FSE for both reviewers ($p < 0.0001$) (Table 3). Among the evaluated abnormal findings, joint effusions were significantly better seen on MAVRIC SL compared with 2D FSE ($p < 0.05$) (Fig. 5). Extraarticular fluid collections communicating with the hip joint were seen only on MAVRIC SL (Fig. 6). Acetabular osteolysis and femoral periprosthetic loosening were also significantly better seen on MAVRIC SL than on 2D FSE for one of the two reviewers ($p < 0.05$). The overall interobserver agreement for the detection of abnormal findings was substantial ($\kappa = 0.762$).

Discussion

MRI of patients with complications from metallic implants has previously been limited by metallic susceptibility artifact. MRI at 1.5 T is usually preferred to 3 T around metal implants regardless of the high-resolution quality of 3-T MRI because image distortion and artifacts are more pronounced at 3 T than at 1.5 T. Increasing receiver bandwidth is one of the strategies to reduce metallic artifacts at higher field strengths, but it cannot be broadened above a certain limit because of the increased specific absorption rate and high cost of MR hardware [23, 24]. To our knowledge, there are no published studies investigating metal artifact reduction at 3 T in patients with joint arthroplasties. The results of our study showed a significant reduction in metal artifact using MAVRIC SL at 3 T in patients with HAs. The measured areas of metal artifact were significantly reduced at both the level of the hip (59.9%) and the femur (31.3%) with MAVRIC SL compared with 2D FSE. In particular, the hip area showed a more dramatic reduction of metal artifact on both the coronal and axial views, and although the exact metallic composition of the hip prostheses was not available to us, the highly concentrated metal component (cobalt chromium) in the hip area (acetabular cup and femoral head) was assumed to result in the pronounced metal artifact seen on 2D FSE. The artifact area of the femur was also significantly decreased with MAVRIC SL on coronal imaging, but there was not a significant difference on axial imaging. The metal artifact around the hip was significantly greater in patients with MOM

THA than in the metal-on-polyethylene group in this study. This difference is likely because of the greater concentration of the large magnetic moment of cobalt chromium in MOM THA compared with the metal-on-polyethylene constructs. The geometry of the implants with regard to head size also has an effect on the metal artifact, but it was not evaluated in this study. The artifact area of the femur did not show a significant difference between the MOM THA group and the metal-on-polyethylene THA group. This lack of a difference is likely because most stems are titanium and thus have a much smaller magnetic moment. The artifact area of the femur was measured at the level of the lesser trochanter, where it is below the maximum location of artifact from the cobalt chromium head.

The joint capsule of the hip and the surrounding anatomic structures were depicted significantly better with MAVRIC SL than with 2D FSE. In particular, MAVRIC SL showed a dramatic improvement in the depiction of the joint capsule and the tendons whose attachment sites were near the joint—namely, the obturator externus and iliopsoas muscles. Visualization of abnormalities in these structures may therefore be possible with MAVRIC SL; MAVRIC SL could be helpful in patients with implant instability by depicting structural compromise of the joint capsule or surrounding structures. In addition, the metal artifact reduction achieved with MAVRIC SL likely contributes to the increased diagnostic confidence at 3-T MRI in this study. The mean level of diagnostic confidence was above 4 for both reviewers, meaning that overall diagnosis was possible with greater than mild to moderate confidence on MAVRIC SL even if the 2D FSE images were nondiagnostic.

Abnormal findings were also significantly better seen on MAVRIC SL than on 2D FSE, particularly joint effusions and extracapsular fluid collections communicating with the joint, which are possible findings suggestive of an adverse local tissue reaction [6, 7]. Although extraarticular fluid collections or masses could be detected on 2D FSE, detailed characterization and visualization of communications with the hip were not possible on 2D FSE because of the extensive metal artifact generated around the hip. However, the significantly improved image quality on MAVRIC SL allowed detection of intraarticular abnormalities, such as synovitis, and the presence of communication between the hip joint and extraarticular fluid collections in most cases. In their study of MRI findings in painful MOM HA, Hayter et al. [6] found that one of the most suggestive MR findings of ALVAL was synovitis and that fluid was commonly observed to decompress into adjacent bursa. Therefore, observation of a fluid collection or soft-tissue mass in the region of a bursa or communication with the hip joint could be highly significant in the setting of a painful MOM HA, but these findings could be seen at 3-T on only MAVRIC SL images. Nawabi et al. [25] also studied MR findings of adverse local tissue reaction; they found that the volume of synovitis was correlated with the severity of the adverse local tissue reaction. They concluded that synovial volume on MRI might be a valuable marker in the longitudinal assessment of asymptomatic patients with a MOM hip resurfacing arthroplasty [25]. According to our study, MAVRIC SL could reveal joint effusions significantly better than 2D FSE for both reviewers. MAVRIC SL is expected to be a useful technique for the detection and surveillance of adverse local tissue reaction in patients with MOM THA who undergo imaging on a 3-T MR system. Acetabular osteolysis was also better seen on MAVRIC SL images. The signal void arising from the metallic component of the femoral head and acetabulum on 2D FSE obscured most of the acetabulum, which compromised

visualization of the bone-metal interface and acetabular osteolysis. The significant reduction in susceptibility artifact on MAVRIC SL enabled visualization of the bone-metal interface around the acetabulum and made detection of acetabular osteolysis possible with MAVRIC SL. Femoral periprosthetic loosening was also better seen on MAVRIC SL for for one of the two reviewers. However, the interobserver agreement for femoral periprosthetic loosening was only fair, unlike the interobserver agreement for the other abnormal findings. Correlation with conventional radiographs should be required for the evaluation of femoral periprosthetic loosening.

There are several limitations to this study. First, because of the retrospective study design, only a small number of cases were included in this study; there were a small number of cases because the tissue contrast between 2D FSE and MAVRIC SL had to match for the image sets. The small number of cases might weaken the statistical power of the results, especially for the evaluation of abnormal findings. A study with a large population is needed. Second, a wider FOV is currently required for MAVRIC SL to avoid aliasing artifact, whereas all parameters of 2D FSE were set in a way to reduce metal artifact. Therefore, the FOV and acquisition matrix used for 2D FSE and MAVRIC SL were not always directly comparable. Third, all the abnormal findings analyzed on MRI were not confirmed surgically or pathologically because most patients were treated conservatively.

In conclusion, MAVRIC SL can significantly reduce metal artifact on 3-T MRI compared with 2D FSE in patients with HA, thus enabling improved depiction of anatomic detail and contributing to increased diagnostic confidence. The improved image quality with MAVRIC SL can also improve detection of intraarticular abnormalities such as synovitis or acetabular osteolysis and may show communications between extraarticular fluid collections and the hip joint. In the future, MAVRIC SL is expected to become a routine sequence in 3-T MRI examinations of the hip for the assessment of postoperative complications in patients with HA.

Acknowledgments

References

1. Passias PG, Bono JV. Total hip arthroplasty in the older population. Geriatrics Aging. 2006; 9:535–543.

2. Harris WH. The problem is osteolysis. Clin Orthop Relat Res. 1995; 311:46–53. [PubMed: 7634590]

3. Potter HG, Nestor BJ, Sofka DM, Ho ST, Peters LE, Salvati EA. Magnetic resonance imaging after total hip arthroplasty: evaluation of periprosthetic soft tissue. J Bone Joint Surg Am. 2004; 86:1947–1954. [PubMed: 15342757]

4. Walde TA, Wiland DE, Leung SB, et al. Comparison of CT, MRI, and radiographs in assessing pelvic osteolysis: a cadaveric study. Clin Orthop Relat Res. 2005; 437:138–144. [PubMed: 16056041]

5. Weiland DE, Walde TA, Leung SB, et al. Magnetic resonance imaging in the evaluation of periprosthetic acetabular osteolysis: a cadaveric study. J Orthop Res. 2005; 23:713–719. [PubMed: 16022981]

6. Hayter CL, Gold SL, Koff MF, et al. MRI findings in painful metal-non-metal hip arthroplasty. AJR. 2012; 199:884–893. [PubMed: 22997383]

7. Hayter CL, Koff MF, Potter HG. Magnetic resonance imaging of the postoperative hip. J Magn Reson Imaging. 2012; 35:1013–1025. [PubMed: 22499278]

8. Hayter CL, Korr MF, Shah P, Koch KM, Miller TT, Potter HG. MRI after arthroplasty: comparison of MAVRIC and conventional fast spin-echo techniques. AJR. 2011; 197:W405–W411. [web]. [PubMed: 21862766]

9. Sutter R, Ulbrich EJ, Jellus V, Nittka M, Pfirmann CW. Reduction of metal artifacts in patients with total hip arthroplasty with slice-encoding metal artifact correction and view-angle tilting MR imaging. Radiology. 2012; 265:204–214. [PubMed: 22923720]

10. De Haan R, Campbell PA, Su EP, De Smet KA. Revision of metal-on-metal resurfacing arthroplasty of the hip: the influence of the hip: the influence of malpositioning of the components. J Bone Joint Surg Br. 2008; 90:1158–1163. [PubMed: 18757954]

11. Campbell P, Shimmin A, Walter L, Solomon M. Metal sensitivity as a cause of groin pain in metal-on-metal hip resurfacing. J Arthroplasty. 2008; 23:1080–1085. [PubMed: 18534479]

12. Langton DJ, Jameson SS, Joyce TJ, Hallab NJ, Natu S, Nargol AV. Early failure of metal-on-metal bearings in hip resurfacing and large-diameter total hip replacement: a consequence of excess wear. J Bone Joint Surg Br. 2010; 92:38–46. [PubMed: 20044676]

13. Hart AJ, Satchithananda K, Liddle AD, et al. Pseudotumors in association with well functioning metal-on-metal hip prostheses: a case-control study using three-dimensional computed tomography and magnetic resonance imaging. J Bone Joint Surg Am. 2012; 94:317–325. [PubMed: 22336970]

14. Grammatopolous G, Pandit H, Kwon YM, et al. Hip resurfacings revised for inflammatory pseudotumour have a poor outcome. J Bone Joint Surg Br. 2009; 91:1019–1024. [PubMed: 19651827]

15. Hauptfleisch J, Pandit H, Grammatopoulos G, Gill HS, Murray DW, Ostlere S. A MRI classification of periprosthetic soft tissue masses (pseudotumours) associated with metal-on-metal resurfacing hip arthroplasty. Skeletal Radiol. 2012; 41:149–155. [PubMed: 22159920]

16. Chang EY, McAnally JL, Van Home JR, Wolfson T, Gamst A, Chung CB. Metal-on-metal total hip arthroplasty: do symptoms correlate with MR imaging findings? Radiology. 2012; 265:848–857. [PubMed: 23047842]

17. Koch KM, Brau AC, Chen W, et al. Imaging near metal with a MAVRIC-SEMAC hybrid. Magn Reson Med. 2011; 65:71–82. [PubMed: 20981709]

18. Koch KM, Lorbiecki FE, Hinks RS, King KF. A multispectral three-dimensional acquisition technique for imaging near metal implants. Magn Reson Med. 2009; 61:381–390. [PubMed: 19165901]

19. Lu W, Pauly KB, Gold GE, Pauly JM, Hargreaves BA. SEMAC: slice encoding for metal artifact correction in MRI. Magn Reson Med. 2009; 62:66–76. [PubMed: 19267347]

20. Hargreaves BA, Worters PW, Pauly KB, Koch KM, Gold GE. Metal-induced artifacts in MRI. AJR. 2011; 197:547–555. [PubMed: 21862795]

21. Chen CA, Chen W, Goodman SB, et al. New MR imaging methods for metallic implants in the knee: artifact correction and clinical impact. J Magn Reson Imaging. 2011; 33:1121–1127. [PubMed: 21509870]

22. Landis JR, Koch GG. The measurement of observer agreement for categorical data. Biometrics. 1977; 33:159–174. [PubMed: 843571]

23. Lee MJ, Kim SJ, Lee SA, et al. Overcoming artifacts from metallic orthopedic implants at high-field-strength MR imaging and multi-detector CT. RadioGraphics. 2007; 27:791–803. [PubMed: 17495293]

24. Viano AM, Gronemeyer SA, Haliloglu M, Hoffer FA. Improved MR imaging for patients with metallic implants. Magn Reson Imaging. 2000; 18:287–295. [PubMed: 10745138]

25. Nawabi DH, Hayter CL, Su EP, et al. Magnetic resonance imaging findings in symptomatic versus asymptomatic subjects following metal-on-metal hip resurfacing arthroplasty. J Bone Joint Surg Am. 2013; 95:895–902. [PubMed: 23677356]
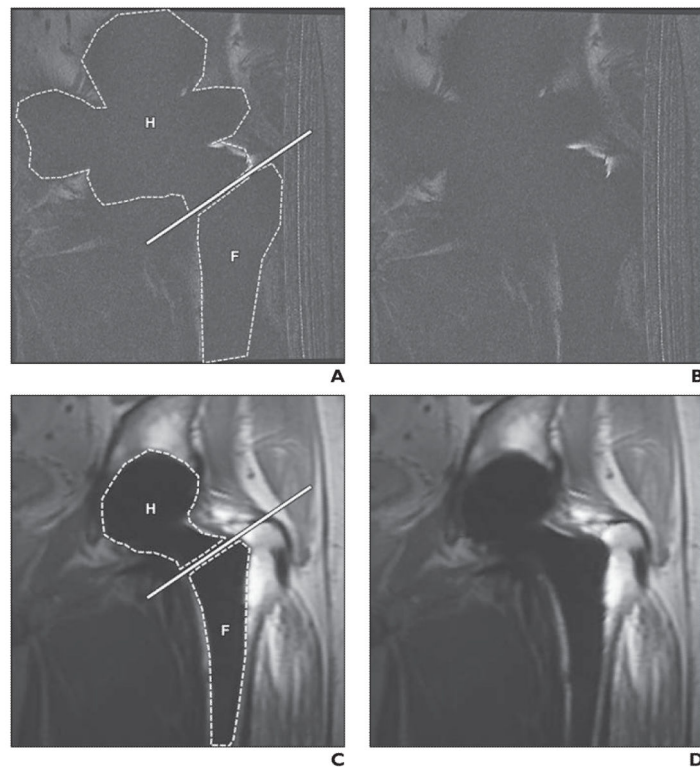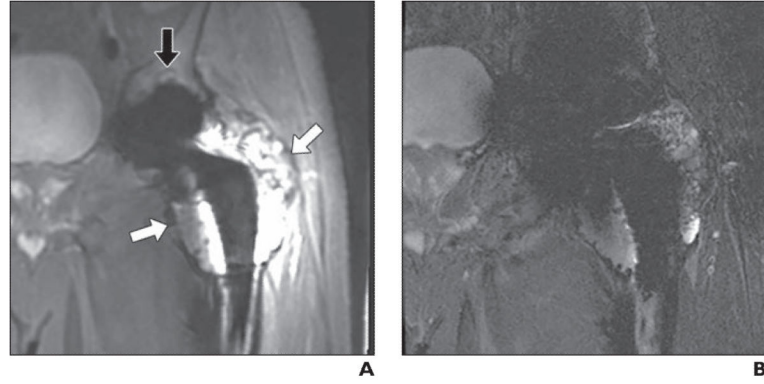
Fig. 1.
45-year-old man with metal-on-metal total hip arthroplasty.

A–D, Comparable coronal 2D fast spin-echo (FSE) (**A** and **B**) and coronal multiacquisition variable-resonance image combination selective (MAVRIC SL) (**C** and **D**) images. Dashed lines in **A** and **C** indicate measured artifact areas in hip (H) and femur (F), and solid lines in **A** and **C** indicate basicervical femoral neck line. Artifact areas of hip and femur at 2D FSE (**A**) are larger than those at MAVRIC SL (**C**). Bone-metal interface is not visualized on 2D FSE (**B**) but is well depicted on MAVRIC SL (**D**). Artifact score was 5 (severe artifact and nonvisualization of bone-metal interface) on 2D FSE (**B**) and 2 (visible artifacts but well-visualized bone-metal interface) on MAVRIC SL (**D**) for both reviewers. There is incidental artifact (radiofrequency artifact) on right side of FSE images (**A** and **B**).
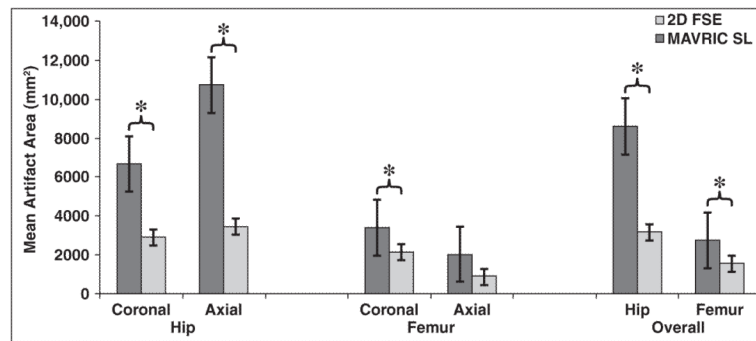
Fig. 2.
Bar graph shows differences in mean artifact areas at hip and femur with 2D fast spin-echo (FSE) and multiacquisition variable-resonance image combination selective (MAVRIC SL) sequences. Measured metallic artifact areas are significantly smaller at MAVRIC SL compared with 2D FSE at level of both hip and femur ($p < 0.0001$). Asterisks indicate statistically significant differences ($p < 0.05$).

Fig. 3.
68-year-old man with left metal-on-metal total hip arthroplasty. Clear cell chondrosarcoma was incidentally found in femoral head specimen. **A** and **B**, Matched coronal multiacquisition variable-resonance image combination selective (MAVRIC SL) inversion recovery (**A**) and 2D fast-spin echo (FSE) STIR (**B**) images. Recurrent tumor (*white arrows*, **A**) in left proximal femur is seen on both MAVRIC SL (**A**) and 2D FSE (**B**) images. However, extent of mass is more clearly identified on MAVRIC SL (**A**). Diagnostic confidence of this image set was 3 (diagnosis can be made on 2D FSE but is better seen on MAVRIC SL) for both reviewers. Small acetabular osteolysis (*black arrow*, **A**) is also revealed only on MAVRIC SL.
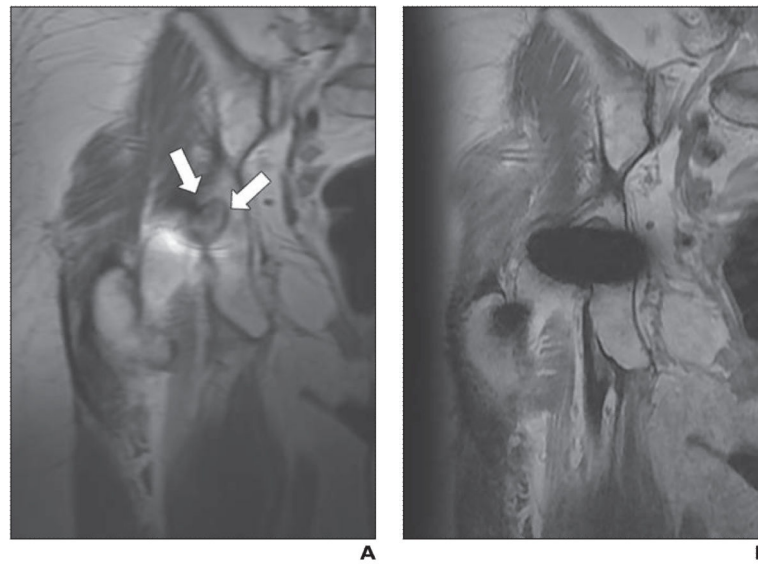
Fig. 4.
73-year-old woman with right metal-on-polyethylene total hip arthroplasty. **A** and **B**, Matched coronal proton density–weighted images of multiacquisition variable-resonance image combination selective (MAVRIC SL) (**A**) and 2D FSE (**B**) sequences. Well-demarcated, lobulated, intermediate-signal-intensity lesion (*arrows*, **A**) is clearly seen in right ischium on MAVRIC SL (**A**), suggesting osteolysis, but lesion is obscured by metal artifact on 2D FSE image (**B**). Diagnostic confidence of this image set was 5 (diagnosis cannot be made on 2D FSE but can be confidently made on MAVRIC SL) for both reviewers.
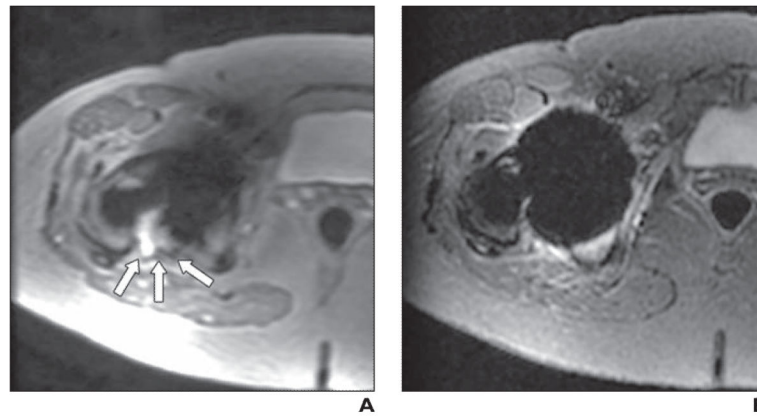
Fig. 5.
55-year-old woman with right metal-on-metal total hip arthroplasty who had elevated serum levels of chromium and cobalt.

A and **B**, Matched axial multiacquisition variable-resonance image combination selective (MAVRIC SL) inversion recovery (**A**) and 2D fast spin-echo (FSE) STIR (**B**) images. Joint effusion with capsular bulging (*arrows*, **A**) is seen in posterior aspect of right hip joint on MAVRIC SL but is not seen on 2D FSE. Diagnostic confidence of this image set was 5 (diagnosis cannot be made on 2D FSE but can be confidently made on MAVRIC SL) for both reviewers. Hip replacement was revised based on MR findings. Surgical diagnosis was adverse local tissue reaction. Foreign body reaction with chronic inflammation was identified in joint.
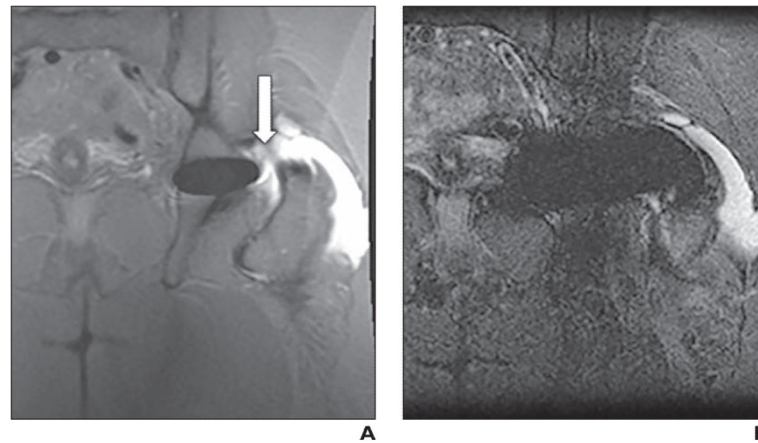
Fig. 6.
60-year-old woman with adverse local tissue reaction after resurfacing arthroplasty of left hip.

A and **B**, Matched coronal multiacquisition variable-resonance image combination selective (MAVRIC SL) inversion recovery (**A**) and 2D fast spin-echo (FSE) STIR (**B**) images. Extraarticular fluid collection (*arrow*, **A**) is seen adjacent to lateral aspect of greater trochanter in region of trochanteric bursa and is shown to communicate with hip joint on MAVRIC SL. Communication with hip is not seen on 2D FSE. Level of diagnostic confidence was 3 (diagnosis can be made on 2D FSE but is better seen on MAVRIC SL) for both reviewers. Patient subsequently underwent surgery. Necrosis and defect were identified in fascia lata and hip joint. Metallic debris and foreign body reaction were found in trochanteric bursa.

TABLE 1

Mean Artifact Scores of 2D Fast-Spin Echo (FSE) Images Versus Multiacquisition Variable-Resonance Image Combination Selective (MAVRIC SL) Images for 25 Matched Image Sets

| Anatomy Imaged and Imaging Plane | Mean Artifact Score (± SD) | | p |
	2D FSE	MAVRIC SL	
Hip			
Coronal			
Reviewer 1	4.92 ± 0.28	2.77 ± 0.73	0.0002[a]
Reviewer 2	5.00 ± 0.00	2.62 ± 0.51	0.0002[a]
Axial			
Reviewer 1	4.92 ± 0.29	2.58 ± 0.79	0.0005[a]
Reviewer 2	4.92 ± 0.29	2.67 ± 0.49	0.0005[a]
Femur			
Coronal			
Reviewer 1	4.69 ± 0.48	2.23 ± 0.60	0.0002[a]
Reviewer 2	4.38 ± 0.51	1.85 ± 0.38	0.0002[a]
Axial			
Reviewer 1	4.58 ± 0.67	2.92 ± 1.24	0.0029[a]
Reviewer 2	4.58 ± 0.51	2.00 ± 0.00	0.0005[a]
Overall			
Hip			
Reviewer 1	4.92 ± 0.28	2.68 ± 0.75	< 0.0001[a]
Reviewer 2	4.96 ± 0.20	2.64 ± 0.49	< 0.0001[a]
Femur			
Reviewer 1	4.64 ± 0.57	2.56 ± 1.00	< 0.0001[a]
Reviewer 2	4.48 ± 0.51	1.92 ± 0.28	< 0.0001[a]

Note—Artifact was scored by two reviewers on a 5-point scale from 1 (normal or barely visible artifact) to 5 (severe artifact and nonvisualization of bone-metal interface).

[a]Statistically significant difference ($p < 0.05$).

TABLE 2

Mean Scores of Depiction of Anatomic Detail on 2D Fast-Spin Echo (FSE) Images Versus Multiacquisition Variable-Resonance Image Combination Selective (MAVRIC SL) Images for 25 Matched Image Sets

Imaging Plane and Anatomy Assessed	Mean Score of Depiction of Anatomic Detail (± SD)		p [a]
	2D FSE	**MAVRIC SL**	
Coronal (n = 13)			
Hip joint capsule			
Reviewer 1	1.15 ± 0.38	2.31 ± 0.75	0.0010[b]
Reviewer 2	1.08 ± 0.28	2.77 ± 0.44	0.0002[b]
Gluteus medius			
Reviewer 1	2.31 ± 0.95	2.85 ± 0.38	0.1094
Reviewer 2	1.92 ± 0.49	3.00 ± 0.00	0.0005[b]
Gluteus minimus			
Reviewer 1	2.08 ± 0.95	3.00 ± 0.00	0.0156
Reviewer 2	1.92 ± 0.49	3.00 ± 0.00	0.0005[b]
Obturator externus			
Reviewer 1	1.08 ± 0.28	2.15 ± 0.99	0.0078[b]
Reviewer 2	1.38 ± 0.51	2.38 ± 0.51	0.0010[b]
Axial (n = 12)			
Hip joint capsule			
Reviewer 1	1.22 ± 0.78	2.50 ± 0.80	0.0078[b]
Reviewer 2	1.17 ± 0.58	2.5 ± 0.52	0.0010[b]
Gluteus medius			
Reviewer 1	2.00 ± 0.95	3.00 ± 0.00	0.0156
Reviewer 2	1.67 ± 0.49	3.00 ± 0.00	0.0005[b]
Gluteus minimus			
Reviewer 1	1.92 ± 0.90	3.00 ± 0.00	0.0078[b]
Reviewer 2	1.67 ± 0.49	3.00 ± 0.00	0.0005[b]
Iliopsoas			
Reviewer 1	1.25 ± 0.62	2.33 ± 0.78	0.0078[b]
Reviewer 2	1.08 ± 0.29	2.42 ± 0.51	0.0005[b]

Note—The depiction of anatomic detail was evaluated by two reviewers on a 3-point scale from 1 (well depicted) to 3 (not visualized).

[a] After Bonferroni correction for multiple comparisons, $p < 0.0125$ shows a statistically significant difference.

[b] Statistically significant difference.

TABLE 3

Abnormal Findings Detected on 2D Fast-Spin Echo (FSE) Images Versus Multiacquisition Variable-Resonance Image Combination Selective (MAVRIC SL) Images for 25 Matched Image Sets

Abnormal Findings	2D FSE (No. of Hips)	MAVRIC SL (No. of Hips)	κ	p
Acetabular osteolysis			0.834	
Reviewer 1	0	7		0.0156[a]
Reviewer 2	1	6		0.0625
Femoral periprosthetic loosening			0.294	
Reviewer 1	1	4		0.25
Reviewer 2	4	11		0.0391[a]
Joint effusion			0.896	
Reviewer 1	2	10		0.0078[a]
Reviewer 2	2	12		0.0002[a]
Extraarticular fluid collection or mass			0.905	
Reviewer 1	7	9		0.500
Reviewer 2	5	9		0.125
Extraarticular fluid collection communicating with the hip joint			0.779	
Reviewer 1	0	4		0.125
Reviewer 2	0	6		0.0313[a]
Tumorlike lesion			1.000	
Reviewer 1	1	1		NA
Reviewer 2	1	1		NA
High-grade muscle or tendon tear			0.898	
Reviewer 1	1	4		0.250
Reviewer 2	1	5		0.125
Other abnormal findings				
Reviewer 1	0	2		0.500
Reviewer 2	0	1		1.000
All abnormal findings			0.762	
Reviewer 1	12	41		< 0.0001[a]
Reviewer 2	14	51		< 0.0001[a]

Note—NA = not applicable.

[a]Statistically significant difference ($p < 0.05$).